

DISCLAIMER

This report was prepared as an account of work sponsored by an agency of the United States Government. Neither the United States Government nor any agency thereof, nor any of their employees, makes any warranty, express or implied, or assumes any legal liability or responsibility for the accuracy, completeness, or usefulness of any information, apparatus, product, or process disclosed, or represents that its use would not infringe privately owned rights. Reference herein to any specific commercial product, process, or service by trade name, trademark, manufacturer, or otherwise, does not necessarily constitute or imply its endorsement, recommendation, or favoring by the United States Government or any agency thereof. The views and opinions of authors expressed herein do not necessarily state or reflect those of the United States Government or any agency thereof.

Printed in the United States of America. Available from:
National Technical Information Service
U.S. Department of Commerce
5285 Port Royal Road
Springfield, VA 22161

NTIS price codes

Paper copy: **A03**

Microfiche copy: **A01**

OIL RECOVERY BY IMMISCIBLE CO₂ FLOODING

Topical Report

By
Frank T. H. Chung

March 1988

Work Performed Under Cooperative Agreement No. FC22-83FE60149

Prepared for
U.S. Department of Energy
Assistant Secretary for Fossil Energy

Jerry F. Casteel, Project Manager
Bartlesville Project Office
P.O. Box 1398
Bartlesville, OK 74005

Prepared by
IIT Research Institute
National Institute for Petroleum and Energy Research
P.O. Box 2128
Bartlesville, OK 74005

TABLE OF CONTENTS

	<u>Page</u>
Abstract.....	1
Introduction.....	1
Acknowledgments.....	3
Displacement Mechanisms.....	3
CO ₂ Solubility.....	3
Oil Swelling.....	4
Viscosity Reduction.....	5
Solution Gas Drive.....	5
Hydrocarbon Extraction.....	5
Mass Transfer Process.....	6
Coreflooding Tests.....	9
Experimental Results and Discussions.....	10
Physical Properties of Recombined E. Eucutta Oil.....	10
Core Properties.....	10
Coreflooding Tests.....	12
CO ₂ Flood (Secondary Oil Recovery).....	12
Waterflood.....	12
CO ₂ Flood After Waterflood.....	13
WAG CO ₂ Flood (WAG Ratio = 1:1) After Waterflood.....	13
Conclusions.....	14
References.....	15

TABLES

1. Properties of oil and core.....	11
2. Solution - gas composition.....	11
3. Results of coreflooding tests.....	14

ILLUSTRATIONS

1. Solubility of CO ₂ in Bartlett crude at 75°, 140°, and 200° F.....	16
2. Prediction method of CO ₂ -solubility in dead heavy oils.....	17

ILLUSTRATIONS (continued)

	<u>Page</u>
3. CO ₂ -solubility in dead and live Chaffee oils.....	18
4. Swelling factor for heavy oil.....	18
5. Viscosity reduction as functions of temperature and CO ₂ -saturated pressure.....	19
6. Hydrocarbon extraction from Wilmington oil by supercritical CO ₂	20
7. Hydrocarbon extraction from Chaffee oil by supercritical CO ₂	20
8. Hydrocarbon composition of extracted oil.....	21
9. Apparatus for hydrocarbon extraction study.....	22
10. Apparatus for CO ₂ diffusion study.....	22
11. Soak time.....	23
12. One-dimensional pore model.....	23
13. CO ₂ concentration profiles in water and oil phases and the moving of oil-water interface as function of time.....	24
14. Effect of blocking-water thickness on CO ₂ diffusion rate.....	24
15. Effect of CO ₂ diffusivity in water on oil saturation time.....	25
16. Coreflooding apparatus.....	25
17. Density and viscosity of recombined E. Eucutta oil with/without CO ₂ saturation.....	26
18. Bubble point pressure for recombined E. Eucutta oil.....	27
19. CO ₂ -solubility in E. Eucutta oil.....	28
20. Swelling factor for E. Eucutta oil.....	29
21. Core wrapped with aluminum foil and rubber sleeve.....	30
22. Coreflooding result of secondary CO ₂ flood.....	31
23. Coreflooding result of waterflood for E. Eucutta oil.....	31
24. Coreflooding result of tertiary CO ₂ flood for E. Eucutta oil.....	32
25. Coreflooding result of tertiary CO ₂ WAG flood for E. Eucutta oil....	32

OIL RECOVERY BY IMMISCIBLE CO₂ FLOODING

By Frank T. H. Chung

ABSTRACT

Heavy oil recovery techniques are being developed at the National Institute for Petroleum and Energy Research (NIPER) in Bartlesville, Oklahoma. This report describes the results of studies made to investigate the mechanisms of immiscible CO₂ displacement and of coreflooding tests for East Eucutta oil (Mississippi). The measurements and correlations for the physical properties of heavy oil-CO₂ mixtures previously performed during this investigation have been reported. This report provides additional information about the properties of heavy oil-CO₂ mixtures and more detailed discussion about the mass transfer process and hydrocarbon extraction mechanisms.

In FY87, research was focused on coreflooding tests to assess oil recovery efficiencies and optimize injection strategy. The objective of this project is to investigate the technical feasibility of the immiscible CO₂ flooding process in the East Eucutta oil field. Conventional flooding methods have been tested and results are presented in this report.

INTRODUCTION

Gas displacement methods of enhanced oil recovery (EOR) encompass two types of processes: miscible and immiscible. Gas miscible flooding is currently the fastest-growing EOR technique. Because interfacial tension (IFT) is eliminated when the displacing gas achieves miscibility with reservoir oil, residual oil saturation can be reduced to a minimum.

If the reservoir pressure is below the "minimum miscibility pressure" (MMP) or the reservoir oil contains a high percentage of heavy components (C₇₊), miscibility between CO₂ and oil cannot be achieved. The immiscible gas displacement method is not as attractive as the miscible method because the oil displacement efficiency is not as high. For these low pressure reservoirs, however, CO₂ can still be used to recover additional oil because it can cause crude oils to swell and reduce oil viscosity. Other mechanisms such as hydrocarbon extraction and solution gas (CO₂) drive will also contribute to oil recovery. Carbon dioxide is considered to be an effective displacing gas to achieve the above mechanisms at relatively low pressure.

For heavier crudes (API gravity below 20°), high viscosity is a major constraint in oil recovery and pipeline transportation; therefore, reducing oil viscosity becomes critical. Methods currently being used for viscous oil recovery include thermal methods (steamflooding and in situ combustion) and CO₂ methods. Steamflooding has been widely applied, and the number of immiscible CO₂ projects is small but increasing.

Carbon dioxide immiscible flooding is an alternate method for viscous oil recovery. Recently, interest in this method has increased because of the economics and pollution problems that can be encountered in steamflooding. Field tests, such as those in Arkansas fields (Ritchie field and Lick Creek field)¹⁻² and in Wilmington field in California,³ have demonstrated the applicability of immiscible CO₂ flooding for heavy oil recovery. Several large-scale field applications are in progress; for example, the Bati Raman oil field in Turkey.⁴

Laboratory tests performed from 1948 to 1952 using carbonated water showed that residual oil saturation after carbonated water injection usually was 2 to 26% PV less than that achieved from water injection alone. Oils with gravities of 28° to 50° API were tested under immiscible conditions.⁵

In recent years, many laboratory studies have been focused on heavy oil (gravity lower than 20° API) recovery by CO₂ immiscible displacement.⁶⁻¹⁴ The injection methods have included cyclic CO₂ stimulation, injecting a single CO₂ slug driven by water, and alternating injection of CO₂ and water. Results show that additional oil recovery of 4 to 24% PV after waterflooding can be obtained by CO₂ immiscible displacement.

The National Institute for Petroleum and Energy Research (NIPER) is conducting research to develop improved methods for oil recovery by immiscible CO₂ displacement. The research includes fundamental studies of displacement mechanisms¹⁵ and coreflooding tests for development of an optimal injection method. Heavy oils are the major target of this research.

Heavy oil production will become more important in the future because it constitutes a large percentage of world oil reserves, and newly discovered light-oil reserves are sparse. According to a recent report,¹⁶ world heavy crude resources are estimated to be 877 to 887 billion barrels, and the recoverable reserves are estimated to be about 183 billion barrels with

current technology. The large number of heavy-oil reservoirs provides a significant potential target for enhanced oil recovery (EOR) technology.

ACKNOWLEDGMENTS

This research by the National Institute for Petroleum and Energy Research is supported by the Department of Energy under Cooperative Agreement DE-FC22-83FE60149, and by Amerada Hess Oil Company.

DISPLACEMENT MECHANISMS

In general, for crude oils of gravity lower than 25° API, the miscible-type displacement cannot be achieved. The principal mechanisms believed to contribute to the improvement of oil recovery by immiscible CO₂ displacement are reduction in oil viscosity, oil swelling, solution gas drive, and hydrocarbon extraction. The changes in crude oil properties depend on the solubility of CO₂ in the crude oil. Following are summaries of the physical properties of CO₂-heavy oil mixtures. Details about the measurements and predictions for the properties of heavy oil with and without CO₂ saturation have been presented.^{15,18}

CO₂ Solubility

The solubility of CO₂ in oil decreases as oil API gravity decreases. For oils of gravity lower than 25° API, the solubility of CO₂ seldom exceeds 700 scf/bbl. As shown in figure 1, the solubility of CO₂ in oils depends on temperature and pressure.¹⁷ The solubility of gaseous CO₂ in oil is a strong function of pressure, while the solubility of liquid CO₂ is not so sensitive. As shown by the 75° F curve in figure 1, the solubility of gaseous CO₂ (at pressures below 1,000 psia) increases drastically with pressure, but the solubility curve levels off as pressures became greater than 1,000 psia because the CO₂ is liquefied. The solubilities of gases in liquids normally decrease with an increase of temperature because the gaseous molecules are more volatile at higher temperatures. However, as the pressure increases, liquids become more dense at lower temperatures, that is, molecules in the liquid phase are packed more tightly and, thus, leave less room for gas molecules to enter. Therefore, at high pressure, the solubility of gas in liquid may increase with temperature because of lower liquid density. This

phenomenon is shown in figure 1 where the 200° F isothermal line crosses the 140° F line at pressures above 3,000 psia and the 75° F line at pressures above 4,000 psi.

Figure 2 shows the dependence of CO₂ solubility on oil API gravity, temperature, and pressure. It also shows how to estimate the solubility of CO₂ in dead, heavy oils at a given pressure, temperature, and oil API gravity by drawing a line between the known conditions. As illustrated, the solubility of CO₂ in a 17° API gravity oil at 1,200 psia and 130° F is 380 scf/bbl.

Solution gas (e.g., CH₄) in crude oil will reduce CO₂ solubility, as shown in figure 3. A saturated oil will have little capacity for CO₂ to dissolve in the oil; however, CO₂ will dissolve in the oil and cause CH₄ to be released from solution. Therefore, the solubility of CO₂ in crude oils at reservoir conditions will gradually increase as more CO₂ is injected because of stripping of solution gas by CO₂. The solubility of CO₂ in the dead oil, predicted from figure 2, will be the maximum values.

Oil Swelling

When CO₂ dissolves in oil, the oil volume increases significantly. This increase of oil volume will increase the volume of pore space occupied by the oil, which will allow discontinuous oil droplets trapped in pores to merge with the flowing oil phase, and reduce the quantity of oil trapped in the pores. The degree of increase in oil volume is indicated by the swelling factor, which is defined as the ratio of the volume of CO₂-saturated oil at the saturation pressure and reservoir temperature to the original volume at the same temperature and 1 atmosphere pressure.

The swelling factor is a linear function of the solubility of CO₂, as is shown in figure 4. If the quantity of CO₂ in oil (scf/bbl) is known, then one can estimate the oil volume increase from figure 4. Since the solubility of CO₂ in heavy oil is less than 700 scf/bbl, the increase in volume is less than 25% of the original oil volume. In other words, oil saturation will increase 25%. For lighter crude oils, the magnitude of volume increase is greater because CO₂ solubility is higher than that in heavy oil.

Viscosity Reduction

The major mechanism in the mobilization of viscous oil by CO₂ is viscosity reduction. Carbon dioxide can significantly reduce the viscosity of heavy oil even at relatively low pressures. The magnitude of viscosity reduction depends on the amount of CO₂ dissolved in the oil, the original oil viscosity, temperature, and pressure.

Figure 5 shows the average values of viscosity reduction as a function of saturation pressure for three isotherms. This plot can be used for quick estimation of the viscosity reduction for heavy oils. A more accurate correlation for the prediction of viscosity reduction has been developed and reported.¹⁸

As shown in figure 5, oil viscosity can be reduced by one order of magnitude if the oil is saturated with CO₂ at pressures greater than 1,000 psi. For high-viscosity oils (>1,000 cp), one order of magnitude reduction in viscosity may not be enough to mobilize the crude oil at reservoir conditions. In addition to CO₂ injection, the crude oil may have to be heated to further reduce its viscosity and improve oil mobilization.

Solution Gas Drive

As shown in figure 1, the solubility of CO₂ increases significantly with pressure. If the pressure of a CO₂-saturated oil is reduced, part of the dissolved CO₂ will be released from the oil because of the reduction in solubility. The released gas will push the oil out of pores and can create an oil bank. A sufficient soak time to allow oil to become saturated with CO₂ and a significant pressure reduction during production are required to recover oil by the solution gas drive mechanism.

Hydrocarbon Extraction

Another property of CO₂ is its ability to extract high-molecular-weight compounds from crude oil at supercritical conditions. This is an important mechanism for CO₂ to achieve miscibility with light oils. Experimental results (Figs. 6 and 7) show that hydrocarbon extraction is enhanced at pressures above 1,200 psia. A comparison of the extracted hydrocarbon compositions at various temperatures and pressures is shown in figure 8. The results were obtained by injecting CO₂ into a heavy oil (from Texas Trix-Liz

oil field) and measuring the amount of hydrocarbons carried out by 1 scf of CO₂ gas. The apparatus is shown in figure 9.

MASS TRANSFER PROCESS

In principle, the mechanisms of immiscible CO₂ displacement are based on the modification of oil properties resulting from the dissolution of CO₂ in the oil. To obtain the greatest reduction in viscosity and increase in oil volume and to achieve optimum displacement efficiency, the crude oil must be saturated with CO₂ at the reservoir temperature and pressure conditions.

Owing to the complexity of the formation matrix, the injected CO₂ gas may not mix well with reservoir oil. In most cases, the dissolution of CO₂ into oil is through the process of diffusion. Molecular diffusion is a slow process, especially when a water phase blocks the oil phase from the CO₂ gas.¹⁹ The blocking water phase retards the diffusion of CO₂ into the oil and completely inhibits the transfer of hydrocarbons from the oil phase into the CO₂ phase.

An experimental apparatus (Fig. 10) was used to determine the saturation time for an oil (37.9° API) which was confined in a 5-in.-long capillary. During the diffusion process, the oil volume increases until it reaches saturation. The diffusion rate can be determined from the change in oil volume. In this experiment, two situations were tested: one with a thin water phase sitting between the CO₂ and oil phases, and the other without a water phase. As shown in figure 11, when the CO₂ gas directly contacts the oil phase, less than 2 days is required for CO₂ to saturate the oil in the 5-in.-long capillary. However, when there is a 0.5-in.-thick water phase between the CO₂ and oil phases, more than 8 days are required for the oil to reach saturation.

A mathematical model was developed for the study of the diffusion process. The model was based on an ideal one-dimensional pore structure (Fig. 12). A water phase was sitting between the trapped oil phase and the flowing CO₂ phase. The model assumes no convection in both the water and the oil phases. The diffusion process is governed by the following equations.

In oil phase:
$$D_{SO} \frac{\partial^2 C_{SO}}{\partial x^2} = \frac{\partial C_{SO}}{\partial t}, \quad 0 < x < X_s$$

In water phase:
$$D_{sw} \frac{\partial^2 C_{sw}}{\partial X^2} = \frac{\partial C_{sw}}{\partial t}, X_s < x < L$$

Where: C_{so} and C_{sw} are mass concentrations of CO_2 in oil and water phases, respectively.

D_{so} and D_{sw} are diffusivities of CO_2 in oil and water phases, respectively,

Conservation of mass across the interface requires that:

$$C_{so}(X_s^-) \frac{dX_s}{dt} + D_{so} \frac{\partial C_{so}(X_s^-)}{\partial x} = C_{sw}(X_s^+) \frac{dX_s}{dt} + D_{sw} \frac{\partial C_{sw}(X_s^+)}{\partial x}$$

Assuming phase equilibrium at the interface:

$$C_{so}(X_s^-) = K_{wo} C_{sw}(X_s^+)$$

Boundary conditions:

$$C_{sw}(L) = K_{wf} C_{sf}$$

$$\frac{\partial C_{so}}{\partial x} \Big|_{x=0} = 0$$

Initial conditions:

$$C_{so} = K_{wo} C_{sw}(\text{int.}), 0 \leq x \leq X_s(0), t = 0$$

$$C_{sw} = C_{sw}(\text{int.}), x_s \leq x \leq L, t = 0$$

$$\frac{dX_s}{dt} = 0 \text{ at } t = 0$$

The rate of increase in volume of the oil phase per unit of interfacial area is

$$\left(D_o \frac{\partial C_o}{\partial x} + C_o \frac{dX_s}{dt} \right) \bar{V}_o,$$

where $\bar{V}_o = 0.04644 \text{ m}^3/\text{kg-mol CO}_2$

Thus,

$$\frac{dX_s}{dt} = \left(D_o \frac{\partial C_o}{\partial x} + C_o \frac{dX_s}{dt} \right) \bar{V}_o$$

$$\frac{dX_s}{dt} = \frac{\bar{V}_o D_o \frac{\partial C_o}{\partial x}}{1 - \bar{V}_o C_o}$$

The interface moving speed is

$$X_s(t) = X_s(0) + \bar{V}_o \int_0^{X_s^-} C_o dx + \int_{X_s(0)}^{X_s(t)} C_o dX_s$$

Because of the oil swelling with more dissolved CO₂ the interface between the oil and water phase will gradually move toward the outlet of the pore and push the water out of the pore. With the mathematical model, we can estimate CO₂-concentration profiles in both oil and water phases and the moving of the interface as a function of time (as shown in figure 13). The effect of water thickness on the oil phase saturation time is shown in figure 14 as an example. The diffusion rate of CO₂ into the oil also depends on the diffusivity of CO₂ in both water and oil. The diffusivity is related to fluid viscosity. The diffusivity is lower for a more viscous fluid; thus more time is required for CO₂ to saturate heavy oils (as shown in figure 15). The

diffusivities of CO₂ in oil (D_{SO}) and water (D_{SW}) were estimated by the following correlations:

$$D_{SO} = 1.41 \times 10^{-10} \mu_o^{-0.47}$$

$$D_{SW} = 5.72 \times 10^{-12} T \cdot \mu_w^{-1}$$

The soak period for CO₂ injection is an important parameter in designing an EOR process. When there is sufficient time for diffusion to saturate and swell the oil, high local displacement efficiencies can be achieved.¹⁹ Under reservoir conditions, the CO₂ soak time will be determined by many factors such as pore structure, water saturation, and residual oil distribution. Unfortunately, so little information is available about the mass transfer process in reservoir rocks that the dynamic situation of CO₂ injected into reservoirs still cannot be predicted accurately.

COREFLOODING TESTS

Several coreflooding studies on the displacement of heavy oils by CO₂ immiscible injection have been reported.⁶⁻¹⁴ Most of these core displacement tests were designed to determine displacement efficiency and to optimize injection schemes for oil recovery.

The objective of this project in FY87 was to investigate the technical feasibility of the immiscible CO₂ flooding process in the East Eucutta oil field (Mississippi). The scope of work included; (1) physical properties of E. Eucutta oil determination, (2) core/rock properties determination, and (3) coreflooding tests. The research was focused on coreflooding tests to assess oil recovery efficiencies and optimize injection strategies. According to the research plan, the following conventional flooding methods were tested:

1. CO₂ flood (secondary oil recovery)
2. Waterflood with E. Eucutta brine
3. Continuous CO₂ flood after waterflood
4. CO₂-alternate-brine (1:1 WAG ratio) flood after waterflood
5. CO₂-alternate-brine (2:1 WAG ratio) flood after waterflood
6. CO₂ huff'n'puff

A coreflooding apparatus (Fig. 16) was set up for this project. The apparatus can be operated at pressures to 4,000 psi and temperatures to 200° F.

Experimental Results and Discussions

Physical Properties of Recombined East Eucutta Oil

We received 5 gallons of stock-tank oil and 5 gallons of brine from East Eucutta oil field. The important properties of the stock-tank oil are listed in table 1. Figure 17 shows the density and viscosity of this oil at various pressures and reservoir temperature (152° F) before and after CO₂ saturation. The oil has high asphaltene content (~18 wt%) and is very viscous at room temperature (~400 cp). This stock-tank oil was recombined with solution gas mixture at a GOR about 48 scf/bbl (uncertainty of measurement = ±5 scf/bbl). The solution gas mixture was purchased by NIPER as specified in table 2. The recombined E. Eucutta oil P-V relationship is shown in figure 18. Some properties of this recombined oil have been determined and are listed in table 1. The solubility of CO₂ in the recombined oil is shown in figure 19, and the swelling factor of the oil after saturated with CO₂ is shown in figure 20.

Core Properties

A sample of reservoir sand from the E. Eucutta oil field, which might have been sampled from the surface soil, contained too much clay and debris such as leaves and metals. Therefore, a Berea sandstone core, which had a permeability of about 300 md, was used for coreflooding tests. The rock is preferentially water-wet. The porosity and permeability values are given in table 1. The permeability of the core was determined at room temperature and under 3,500 psig overburden pressure by measuring the gas flow rate and pressure drop across the dry core at 1 atm. outlet pressure. Then the core was flooded with brine at a constant flow rate, and the brine permeability was determined. There is a significant difference (~10 fold) between gas permeability and brine permeability.

TABLE 1. - Properties of East Eucutta oil and Berea sandstone core

A. Stock-tank oil:	
Gravity, °API	22
Viscosity @ 75° F, 1 atm, cp	399
Asphaltene content, wt%	17.85
B. Recombined live oil:	
Density @ 75° F, 2,500 psia, g/cm ³	0.9466
Solution gas-oil ratio, (scf/bbl)	48
Saturation pressure, psig:	
at 75° F	170
at 152° F	250
Thermal expansion factor, TEF	1.05
Formation volume factor, FVF	1.06
C. Core/Rock	
Formation	sandstone
Length, in.	24
Diameter, in.	2
Pore volume, cm ²	240.4
Porosity, %	18.92
Permeability @ 152° F, 2,500 psia, md:	
N ₂	305
brine	27.7

TABLE 2. - Solution gas composition

Component	Mol Percent
Hydrogen sulfide	Nil
Carbon dioxide	1.90
Nitrogen	1.29
Methane	60.20
Ethane	5.49
Propane	12.34
iso-Butane	6.14
n-Butane	6.04
iso-Pentane	2.46
n-Pentane	4.14
	<u>100.00</u>

Coreflooding Tests

The consolidated sandstone was cut into a 2-in. diameter, 2-ft long core. The core was wrapped with aluminum foil and a rubber sleeve (Fig. 21) to prevent CO₂ from diffusing out, and then put into the coreholder with an overburden pressure of 3,500 psig. The core was kept under a constant temperature of 152° F. Flood tests were conducted at constant injection rate with the outlet pressure maintained at 2,500 psig by a backpressure regulator. Before each test run, the Berea sandstone core was flooded with toluene and then displaced first with methanol and then with brine until it was saturated with brine. The brine saturated core was kept at test conditions for about 1 day, then the recombined E. Eucutta oil was injected into the core to displace the brine until no additional brine was produced. Both brine and oil were injected at a constant rate of about 50 cm³/hr. The oil-saturated core was kept at test conditions for at least 1 day. The experimental procedure and results for each test are described as follows:

CO₂ Flood (Secondary Oil Recovery)

The core containing connate water and initial oil saturation was displaced by CO₂. Carbon dioxide gas was injected continuously at a constant injection rate of 5 cm³/hr, which corresponds to a linear velocity of 1 ft/day. Results of this test are shown in figure 22. Ultimate oil recovery was about 55% of original oil in place (OOIP) at 1.2 PV CO₂ injection. The CO₂ utilization factor is about 5.6 Mscf/bbl of additional oil recovered. Gas breakthrough occurred at about 0.2 PV injection. However, after gas breakthrough, there was still a significant amount of oil recovered. E. Eucutta oil recovery by CO₂ flooding was higher than that obtained by waterflooding (Fig. 23). The asphaltene content of the effluent oil was determined, and a slight decrease was noted.

Waterflood

The same core containing connate water and initial oil saturation was waterflooded with E. Eucutta brine. The brine was injected at a higher rate (50 cm³/hr) until a water-cut of 98% was reached. The total brine injected was more than 1.5 PV. Results of this test are shown in figure 23. Water broke through at about 0.6 PV injection, which was much later than CO₂

breakthrough. After water breakthrough, oil production dropped significantly. Total oil recovery by waterflood was only 43% of the OOIP. During brine injection, the pressure difference between inlet and outlet gradually increased to about 450 psi at 0.5 PV injection and then decreased to 280 psi after 1 PV injection.

CO₂ Flood After Waterflood

After waterflooding, the core was kept at 152° F for a period of time until the inlet and outlet pressures recovered to 2,500 psig before starting the injection of CO₂. Carbon dioxide gas was injected at a constant rate of 5 cm³/hr (1 ft/day) until there was no longer a significant amount of oil produced. Results of this test are shown in figure 24. Gas breakthrough occurred at about 0.22 PV injection. At the beginning of CO₂ injection, the displacement was piston-like, and only brine was produced until about 0.2 PV of CO₂ had been injected when oil production began, after which only a trace amount of brine was produced. The tertiary CO₂ flood recovered about 33% OOIP of additional oil with 1.5 PV injection of CO₂ after waterflooding. The carbon dioxide utilization factor was 11.7 Mscf/bbl of additional oil recovered.

CO₂-WAG Flood (WAG Ratio = 1:1) After Waterflood

In this test, the core was waterflooded until the water-cut of the effluent was above 98%. The waterflooded core was then flooded with alternate slugs of CO₂ (0.2 PV) and brine (0.2 PV) until no significant amount of additional oil was produced. Results of this test are shown in figure 25. Oil production by this method is very close to that of continuous CO₂ injection (see fig. 24) up to 1.2 PV injection. However, after 1.2 PV injection, the oil production by the CO₂ WAG injection method was still significant, whereas the oil production by continuous CO₂ flood had already become approximately constant. Additional oil recovery of about 40% OOIP after five injection cycles (2 PV) was obtained by the CO₂-WAG process. Comparing the gas production curves of the CO₂-WAG flood (Fig. 6) and the tertiary CO₂ coreflood (Fig. 5), we can see that the WAG process significantly delayed the breakthrough of gas and an increase in the gas-oil ratio. The utilization of CO₂ is more efficient (CO₂ utilization factor at 1.5 PV injection = 5.9 Mscf/bbl) for the WAG injection method.

CONCLUSIONS

1. The solubility of CO₂ in E. Eucutta oil is 560 scf/bbl at 152° F and 2,500 psig. With this amount of CO₂ dissolved, the volume of the oil can be increased by 20%, and the oil viscosity is reduced to about one-tenth of its original value. This significant change of oil properties is the major reason for high oil recovery by CO₂ immiscible displacement. The estimated minimum miscibility pressure (MMP) of the E. Eucutta oil is about 3,200 psia.

2. From analysis of the asphaltene content of the displaced oil, we found that there is a slight decrease in asphaltene content, which might be the result of asphaltene precipitation by CO₂ inside the core.

3. Results of these coreflooding tests, indicate that the East Eucutta oil field is a good candidate for a CO₂ flood. Oil recoveries in all of these tests are summarized in table 3. The CO₂-WAG process is economically more significant than that of continuous CO₂ flood. Future research will be focused on testing various CO₂ mobility control methods to improve the efficiency of CO₂ immiscible displacement.

TABLE 3. - Results of coreflooding tests

	Oil recovery, % OOIP	
	at 1.2 PV injection	ultimate
1. Secondary CO ₂ flood	55	59
2. Secondary brine flood	43	44
3. Tertiary CO ₂ flood (after brine flood)	31	34
4. Tertiary CO ₂ WAG (1:1) flood (after brine flood)	32	40

REFERENCES

1. Reid, T. B. and H. J. Robinson. Lick Creek Meakin Sand Unit Immiscible CO₂-Waterflood Project. SPE paper 9795, Apr., 1981.
2. Durham, E. N. and J. A. Watson. CO₂ Field Injection Project Conducted by Phillips Petroleum Company-Ritchie Field, Union County, Arkansas. Department of Energy Report No. DOE/MC/08341-17, Oct., 1980.
3. Saner, W. B. and J. T. Patton. CO₂ Recovery of Heavy Oil: The Wilmington Field Test. SPE paper 12082, October 1983.
4. Kantar, K., D. Karaoguz, K. Issever, L. and Varana. Design Concepts of a Heavy-Oil Recovery Process by an Immiscible CO₂ Application. J. Pet. Tech., February 1985, pp. 275-283.
5. Khatib, A. K., R.C. Earlougher, and K. Kantar. CO₂ Injection as an Immiscible Application for Enhanced Recovery in Heavy Oil Reservoirs. SPE paper 9928, March 1981.
6. Sanku, V. and A. S. Emanuel. A Laboratory Study of Heavy Oil Recovery with CO₂ Injection. SPE paper 11692, March 1983.
7. Sanku, V., J. L. Creek, S. S. DiJulio, and A. S. Emanuel. A Laboratory Study of Wilmington Tar Zone CO₂ Injection Project. SPE paper 12751, April 1984.
8. Sanku, V., A. S. Emanuel, and S. S. DiJulio. Recovery of Heavy Oils by CO₂ Injection. Energy Progress, v. 6, No. 2, June 1986, pp. 91-96.
9. Jha, K. N. A Laboratory Study of Heavy Oil Recovery with Carbon Dioxide. Pet. Soc. of CIM paper No. 4, September 1985.
10. Klin, M. A. and S. M. Faroug Ali. Heavy Oil Production by Carbon Dioxide Injection. J. Can. Pet. Tech., September-October 1982, pp. 64-72.
11. Rojas, G. and S. M. Faroug Ali. Dynamics of Subcritical CO₂/Brine Floods for Heavy Oil Recovery. SPE paper 13598, March 1985.
12. Rojas, G. and S. M. Faroug Ali. Scaled Model Studies of Carbon Dioxide/Brine Injection Strategies for Heavy Oil Recovery from Thin Formations. J. Can. Pet. Tech., January-February 1986, pp. 85-93.
13. Sayegh, S. G. and B. B. Maini. Laboratory Evaluation of the CO₂ Huff'n'Puff Process for Heavy Oil Reservoirs. J. Can. Pet. Tech., May-June 1984, pp. 29-36.
14. Mayer, E. H., R. C. Earlougher, Sr., A. Spivak, and A. Costa. An Analysis of Heavy Oil Immiscible CO₂ Tertiary Coreflood Data. SPE/DOE paper 14901, April 1986.

15. Chung, T. H. Heavy Oil Recovery by CO₂ Immiscible Displacement Method. Department of Energy Report No. NIPER-76, 1986.

16. Meyer, R. F. and C. J. Schenk. An Estimate of World Heavy Crude Oil and Natural Bitumen Resources. Pres. at 3rd UNITA Conference, July, 1985, pp. 176-191.

17. Miller, J. S. and R. A. Jones. A Laboratory Study to Determine Physical Characteristics of Heavy Oil after CO₂ Saturation. Department of Energy Report No. DOE/BETC/RI-83/11, January 1984.

18. Chung, F. T. H., R. A. Jones, and H. T. Nguyen. Measurements and Correlations of the Physical Properties of CO₂-Heavy Crude Oil Mixtures. SPE paper 15080, April 1986.

19. Grogan, A. T. and W. V. Pinczewski. The Role of Molecular Diffusion Processes in Tertiary Carbon Dioxide Flooding. SPE/DOE paper 12706, April 1984.

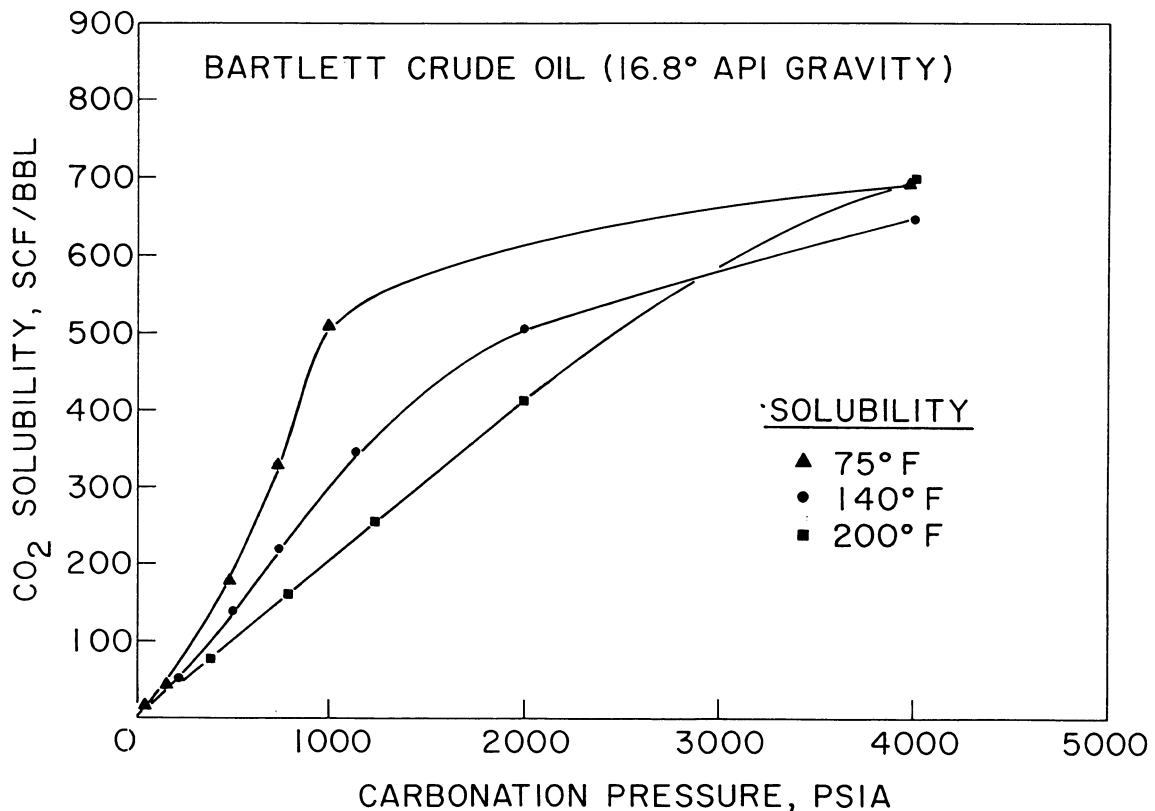


FIGURE 1. - Solubility of CO₂ in Bartlett crude at 75°, 140°, and 200° F.

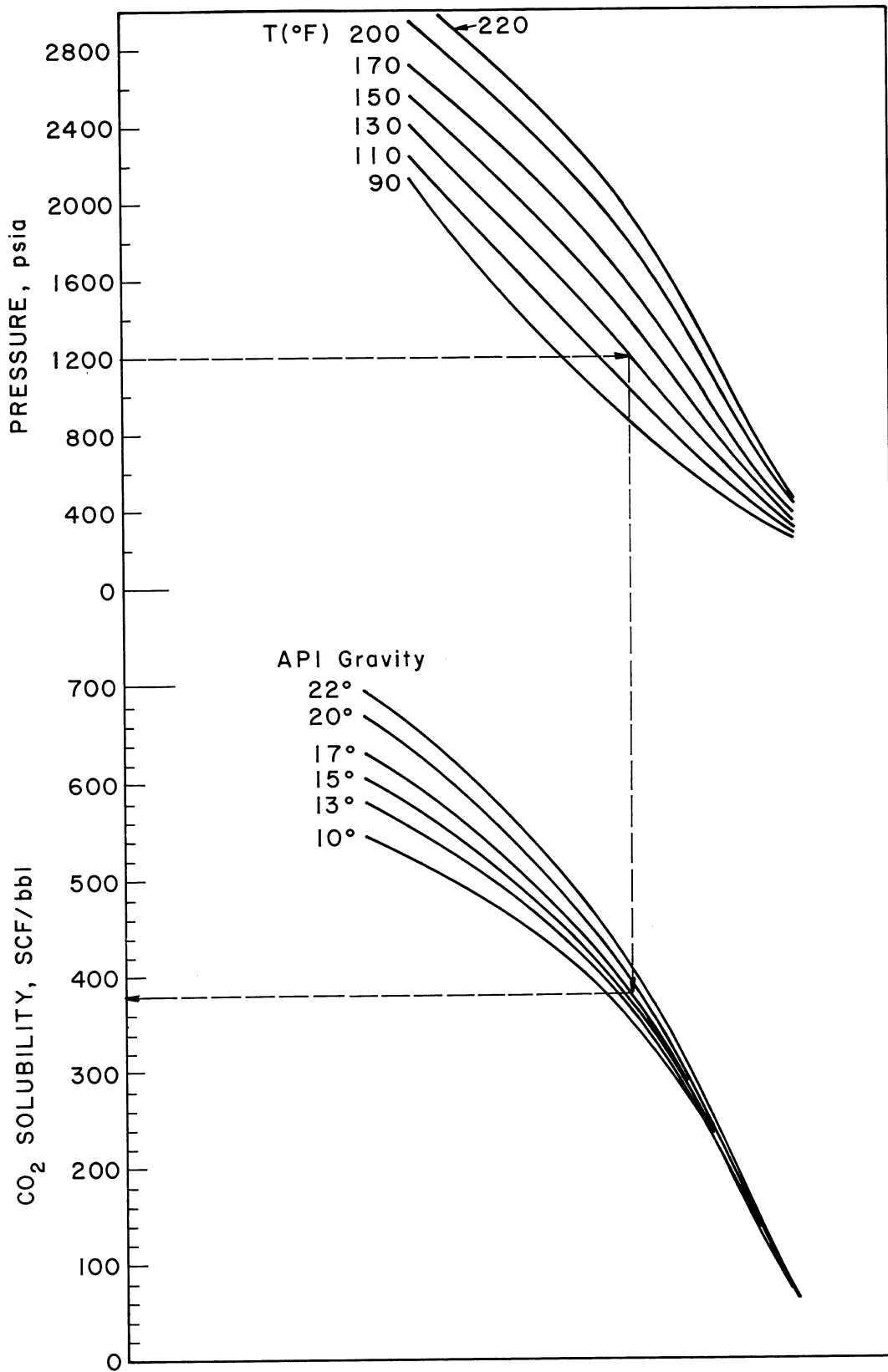


FIGURE 2. - Prediction method of CO₂-solubility in dead heavy oils.

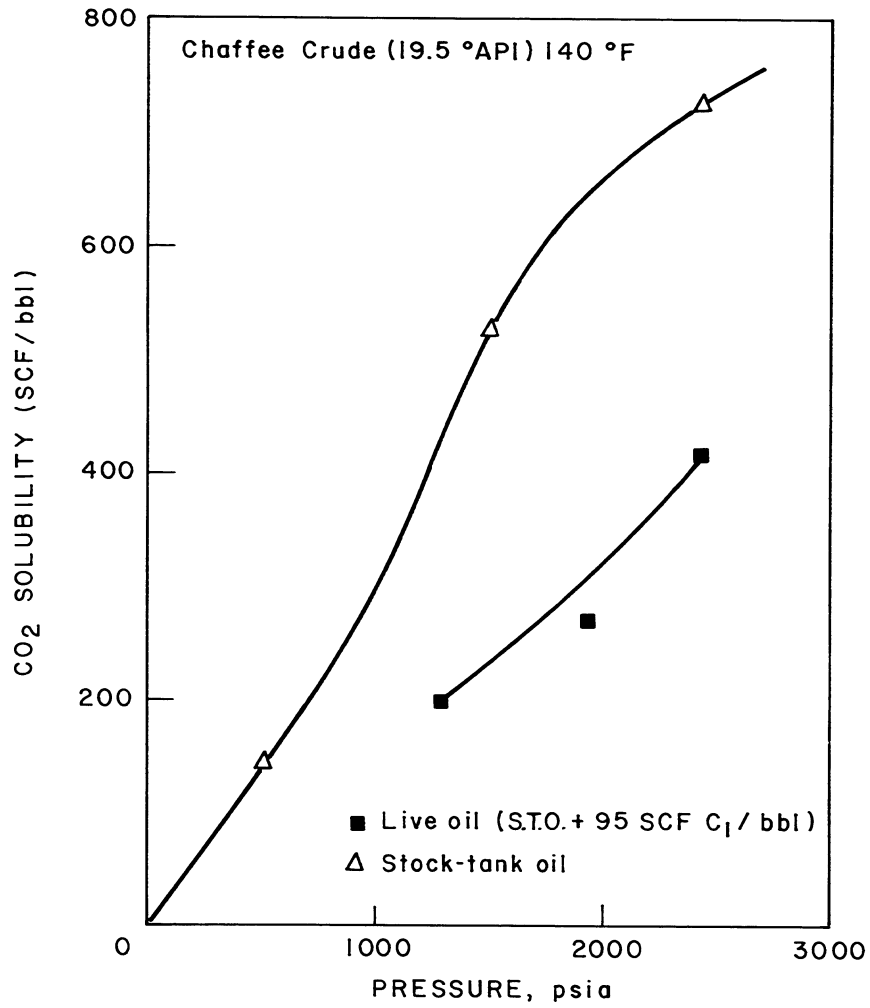


FIGURE 3. - CO₂-solubility in dead and live Chaffee oils.

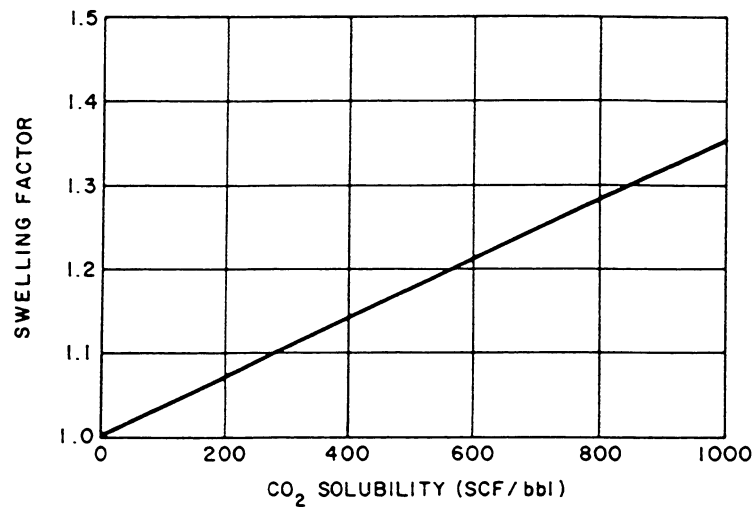


FIGURE 4. - Swelling factor for heavy oil.

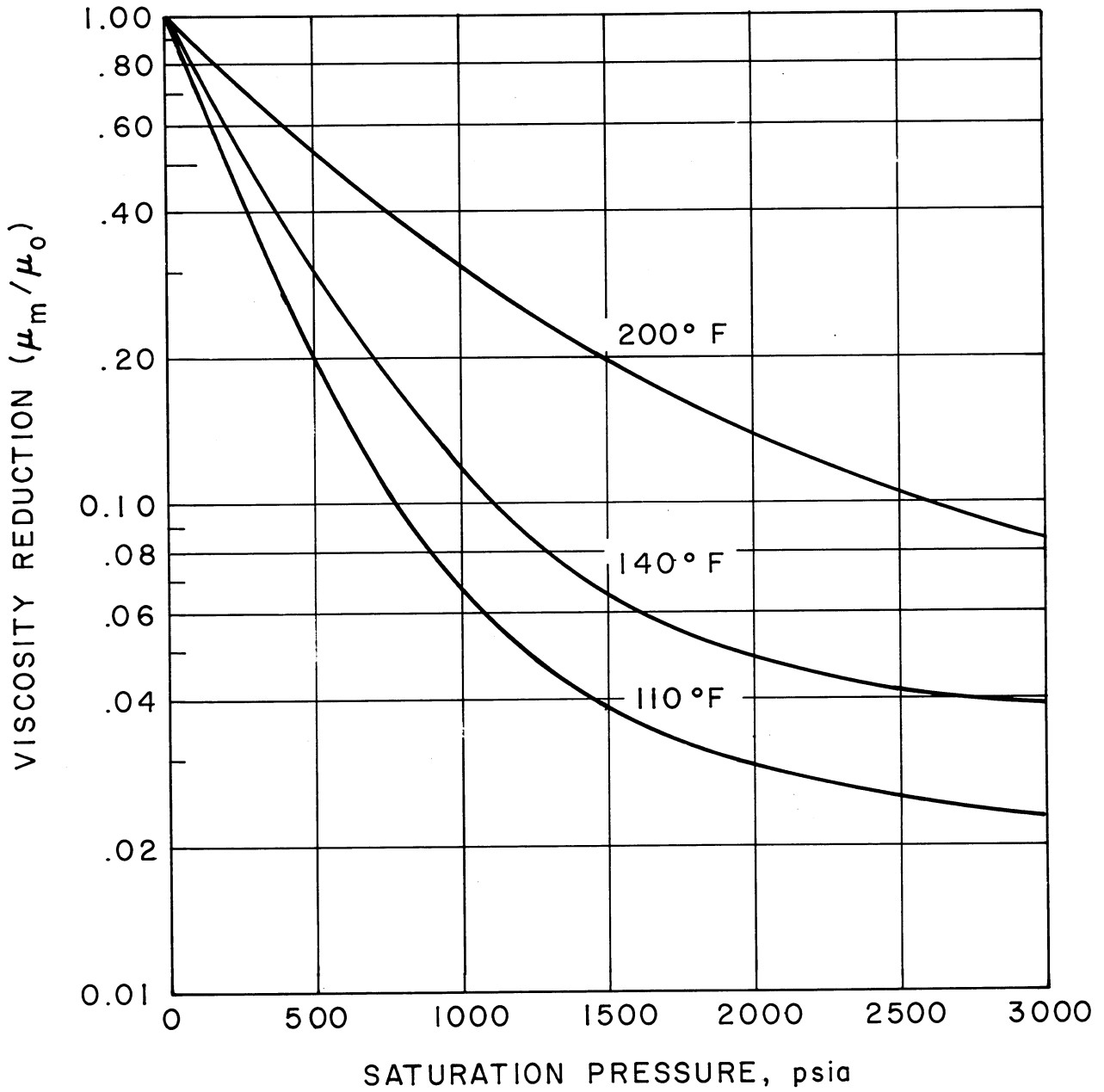


FIGURE 5. - Viscosity reduction as functions of temperature and CO₂-saturated pressure.

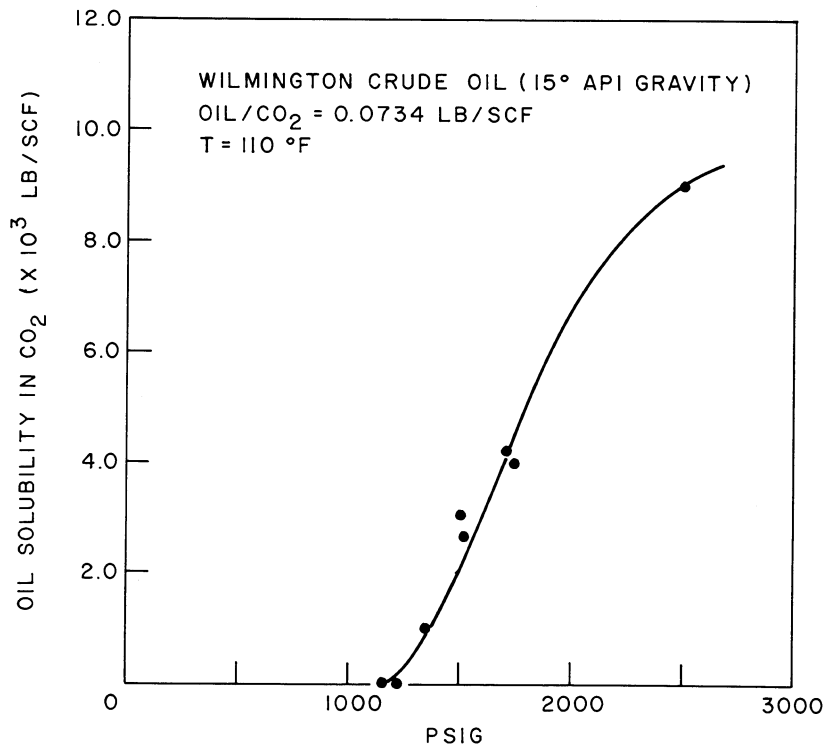


FIGURE 6. - Hydrocarbon extraction from Wilmington oil by supercritical CO₂.

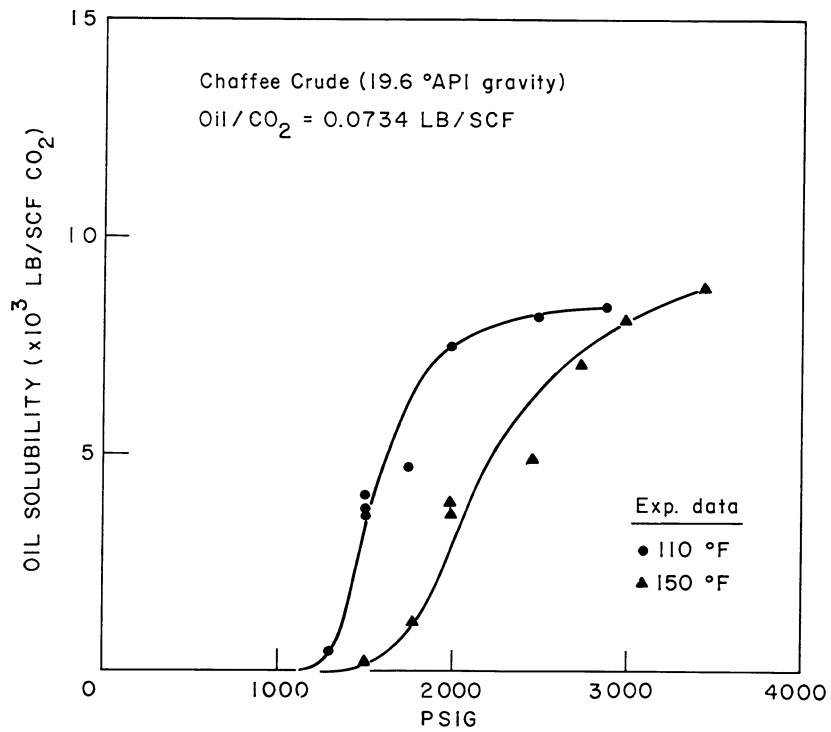


FIGURE 7. - Hydrocarbon extraction from Chaffee oil by supercritical CO₂.

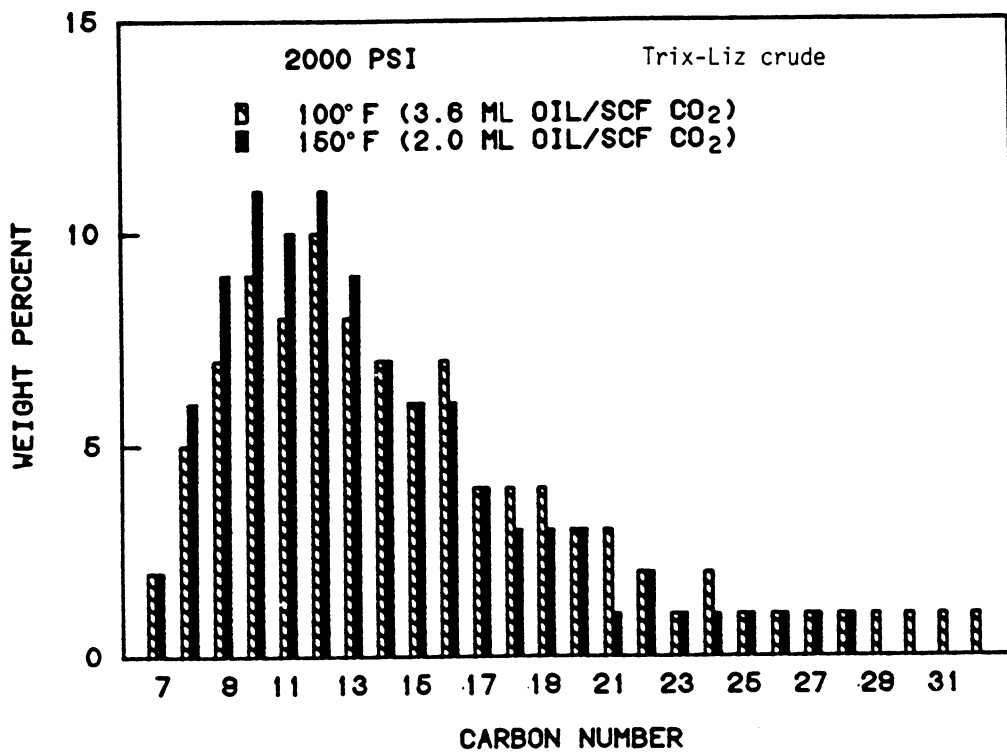
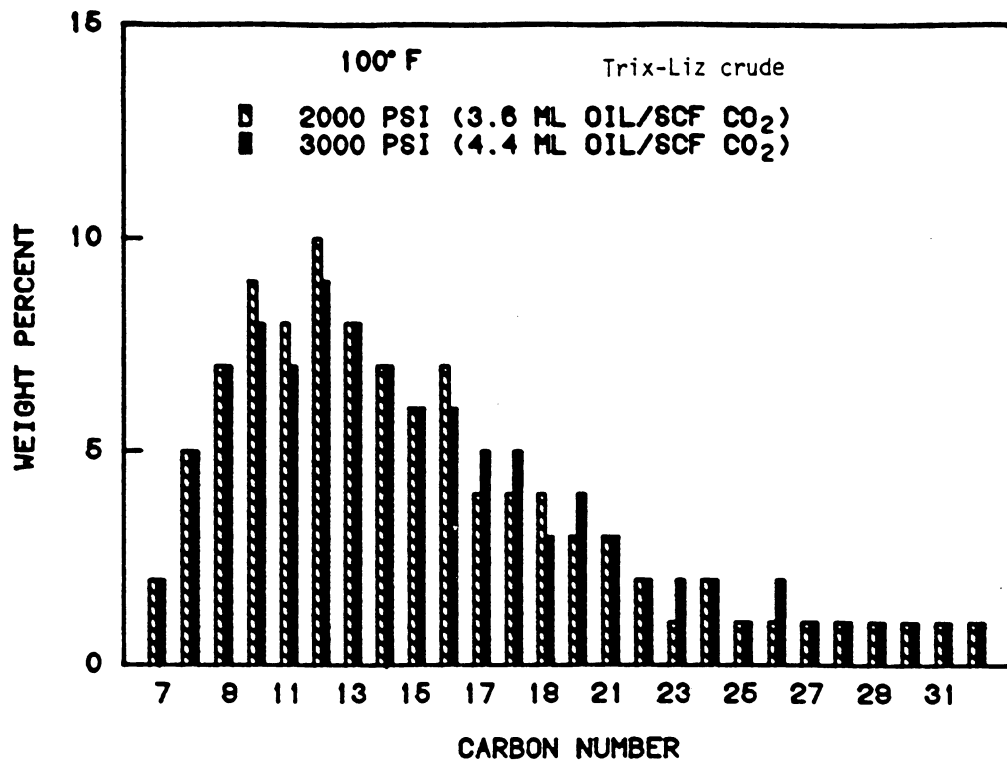


FIGURE 8. - Hydrocarbon composition of extracted oil.

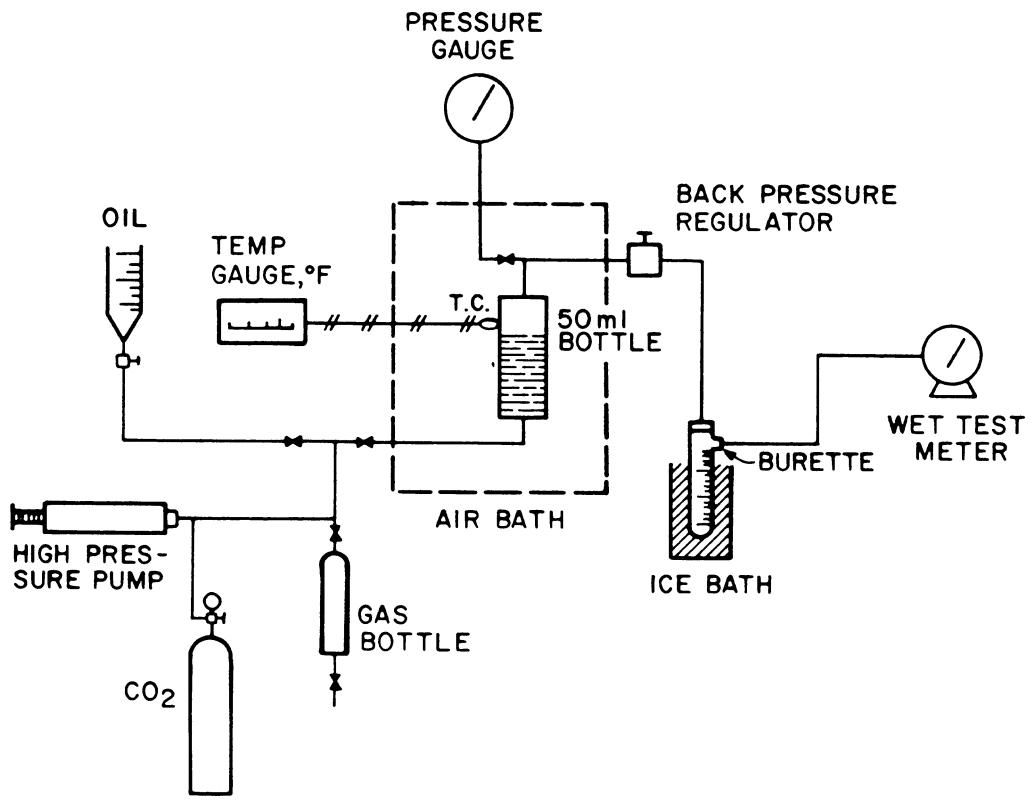


FIGURE 9. - Apparatus for hydrocarbon extraction study.

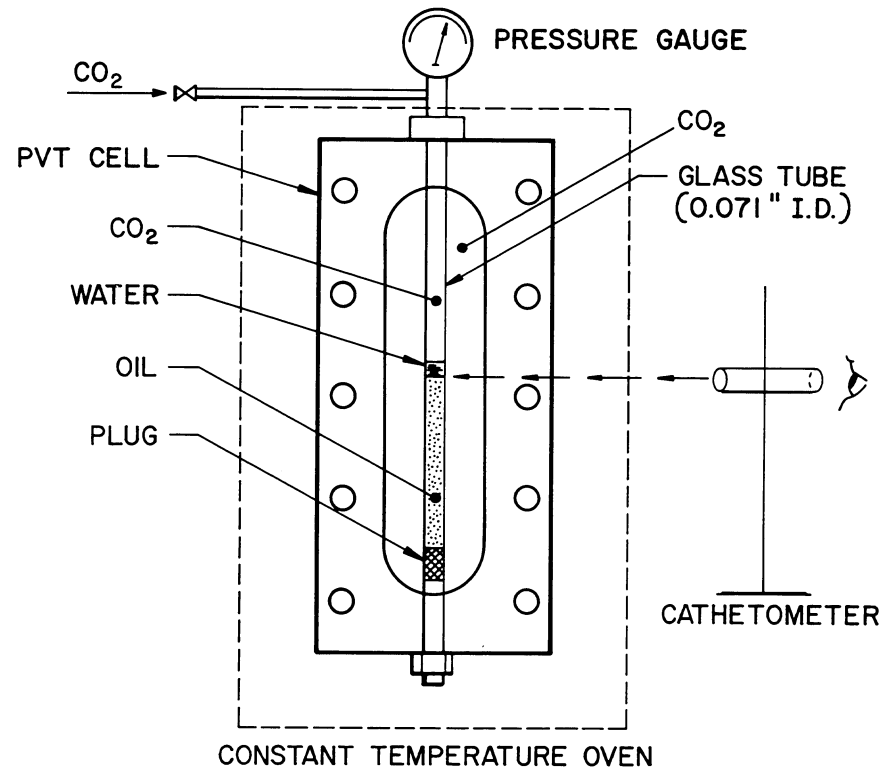


FIGURE 10. - Apparatus for CO₂ diffusion study.

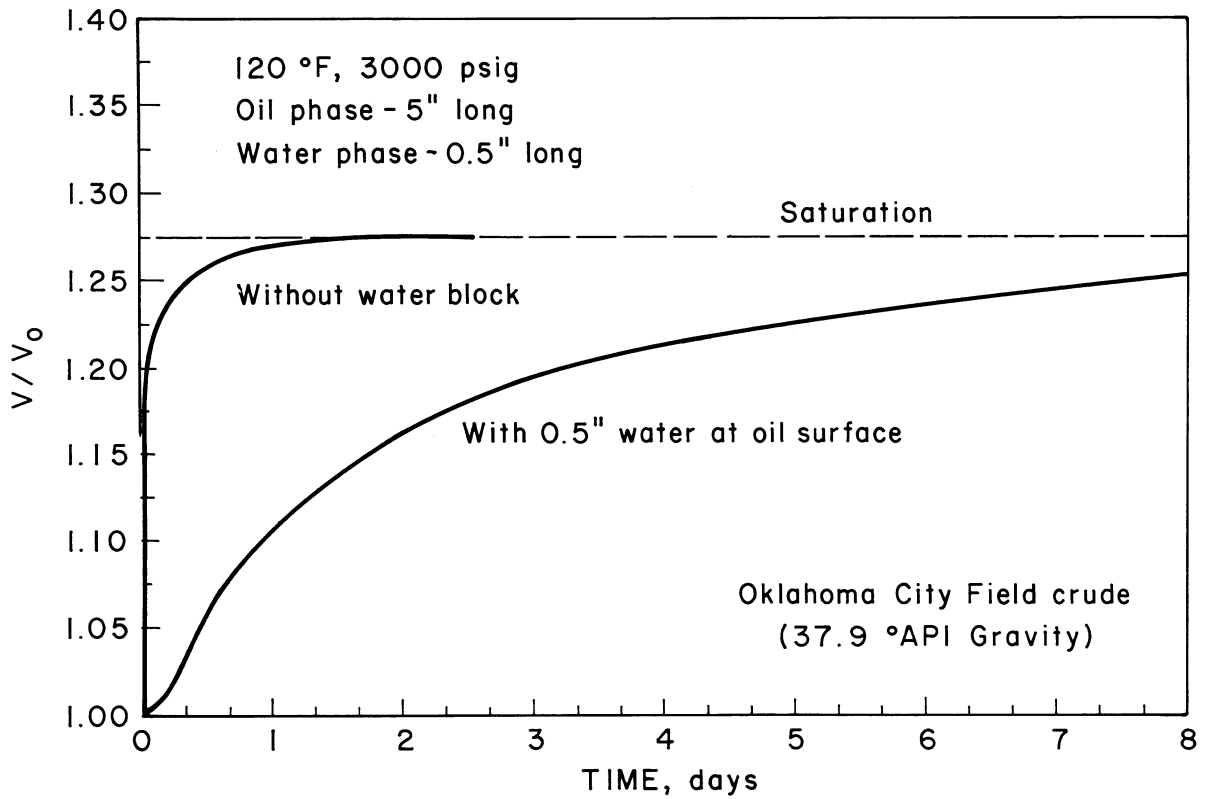


FIGURE 11. - Soak time.

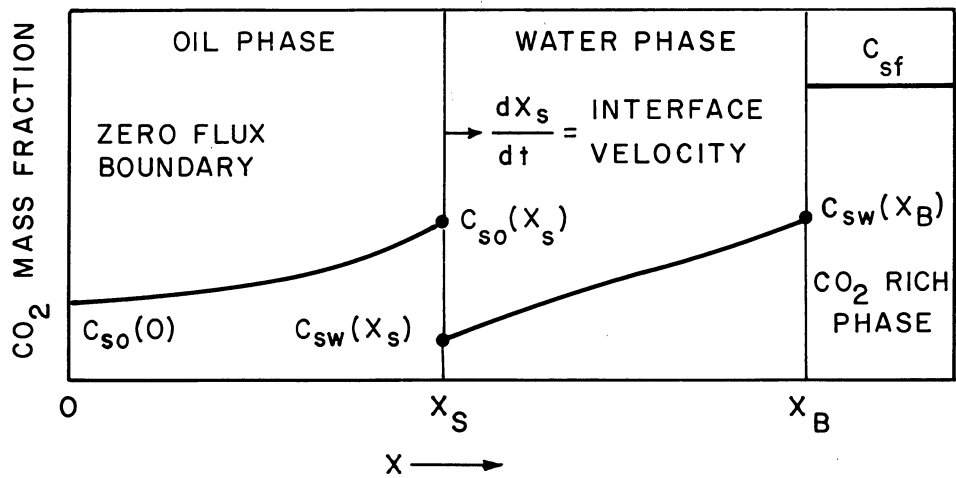


FIGURE 12. - One-dimensional pore model.

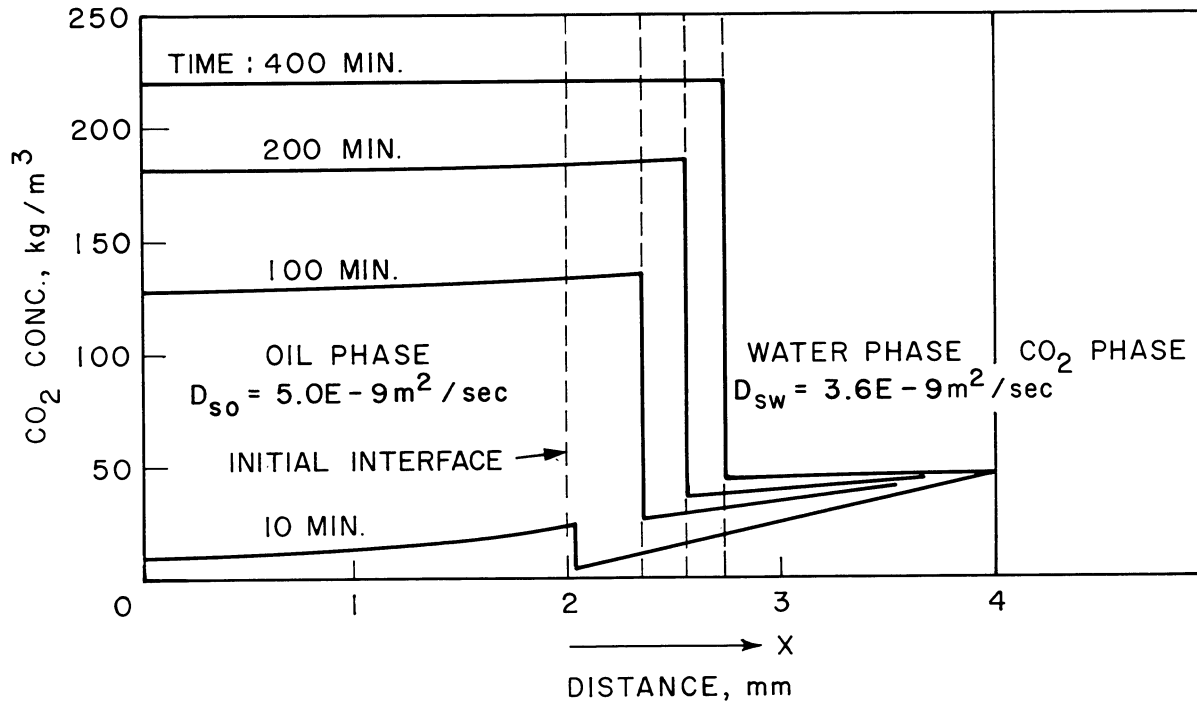


FIGURE 13. - CO₂ concentration profiles in the water and oil phases and the motion of the oil-water interface as a function of time.

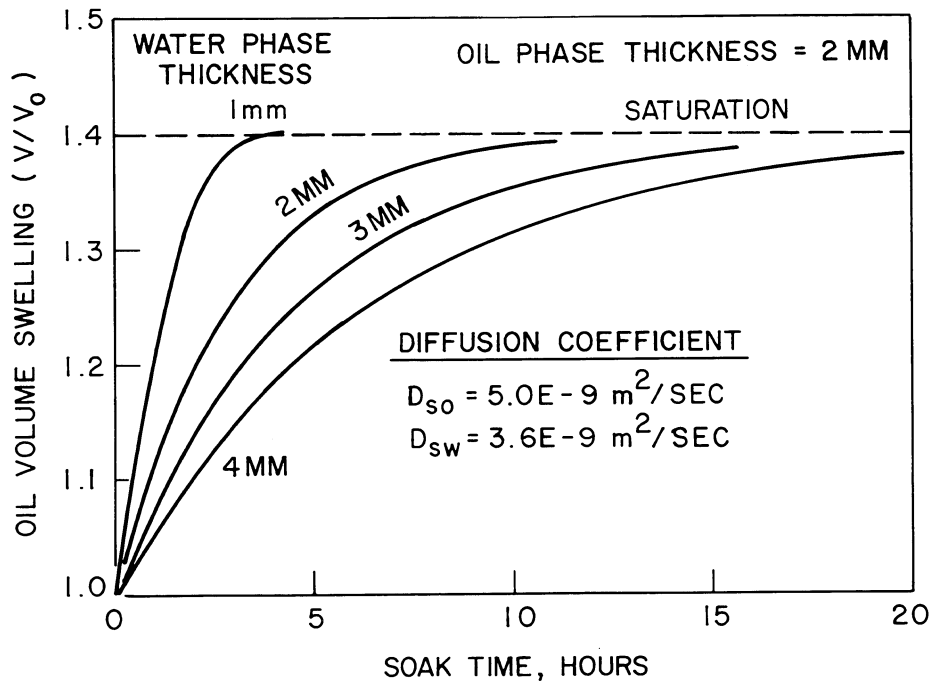


FIGURE 14. - Effect of blocking-water thickness on CO₂ diffusion rate.

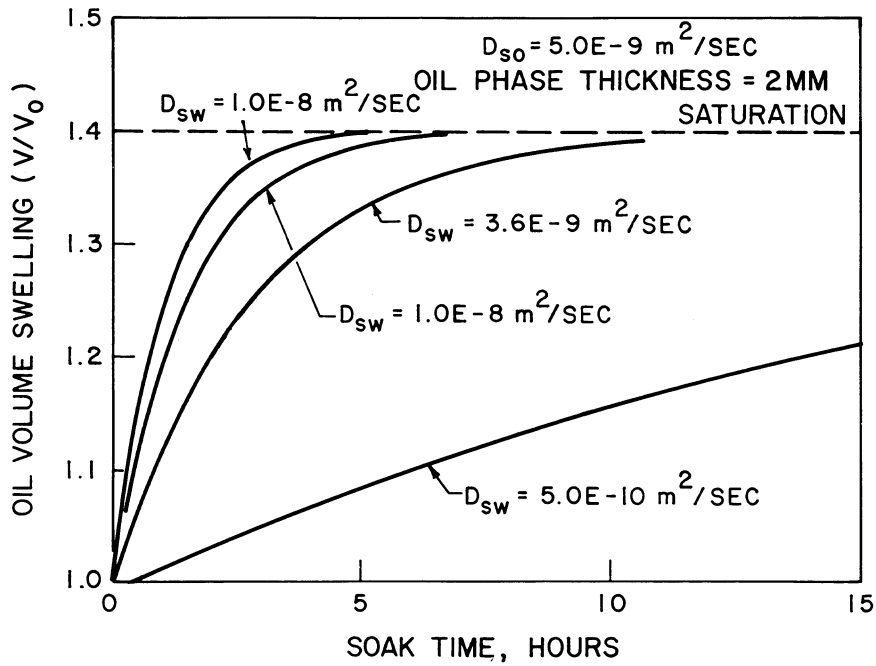


FIGURE 15. - Effect of CO₂ diffusivity in water on oil saturation time.

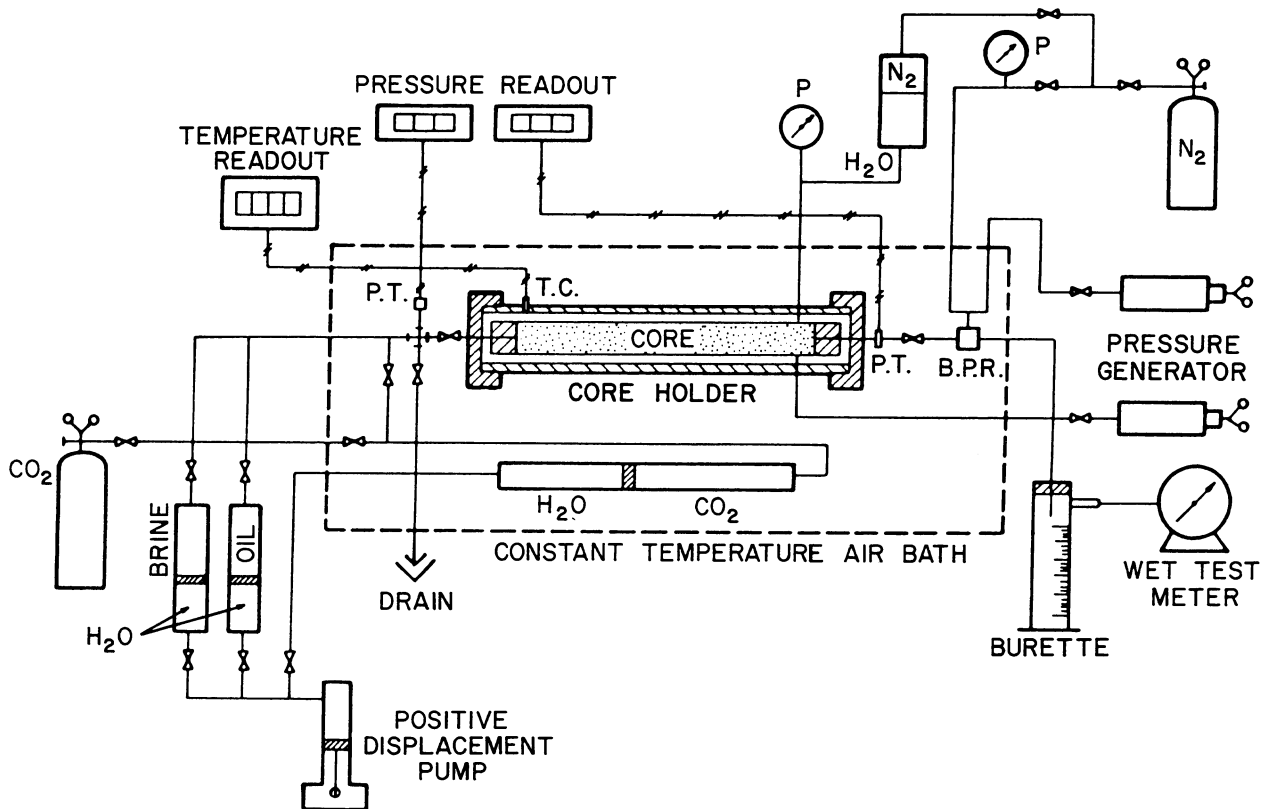


FIGURE 16. - Coreflooding apparatus.

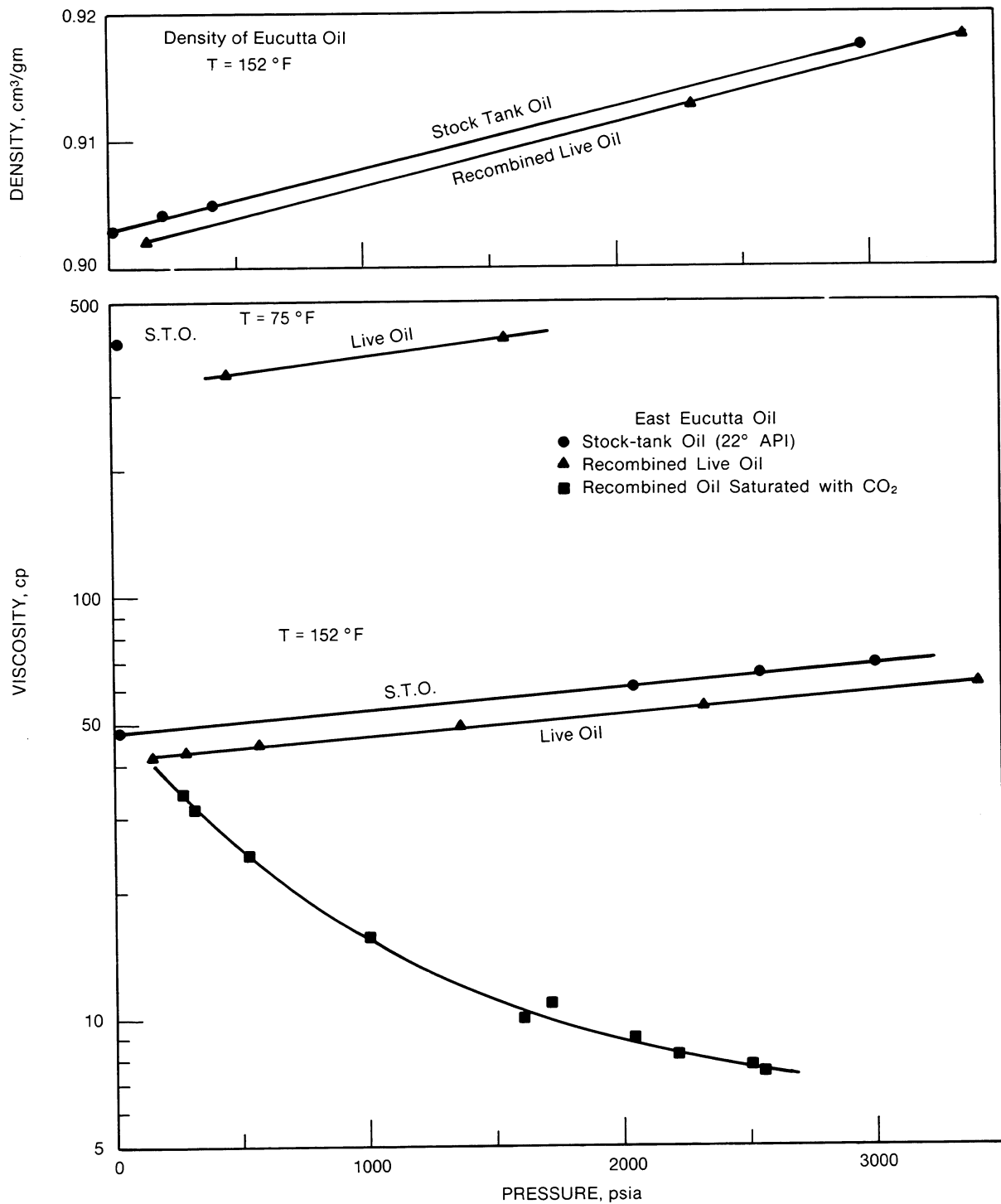


FIGURE 17. - Density and viscosity of recombined E. Eucutta oil with/without CO₂ saturation.

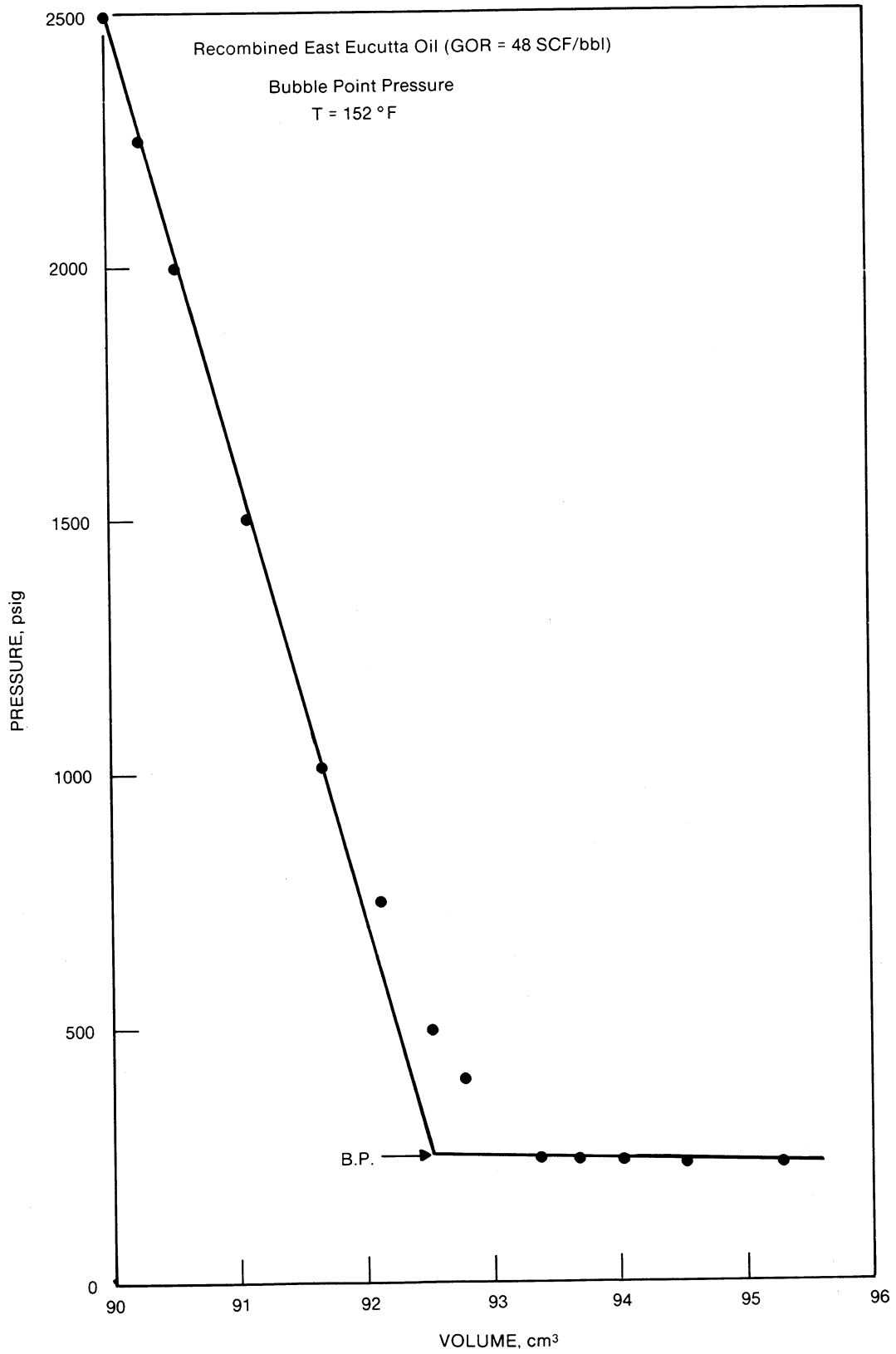


FIGURE 18. - Bubble point pressure for recombined Eucutta oil.

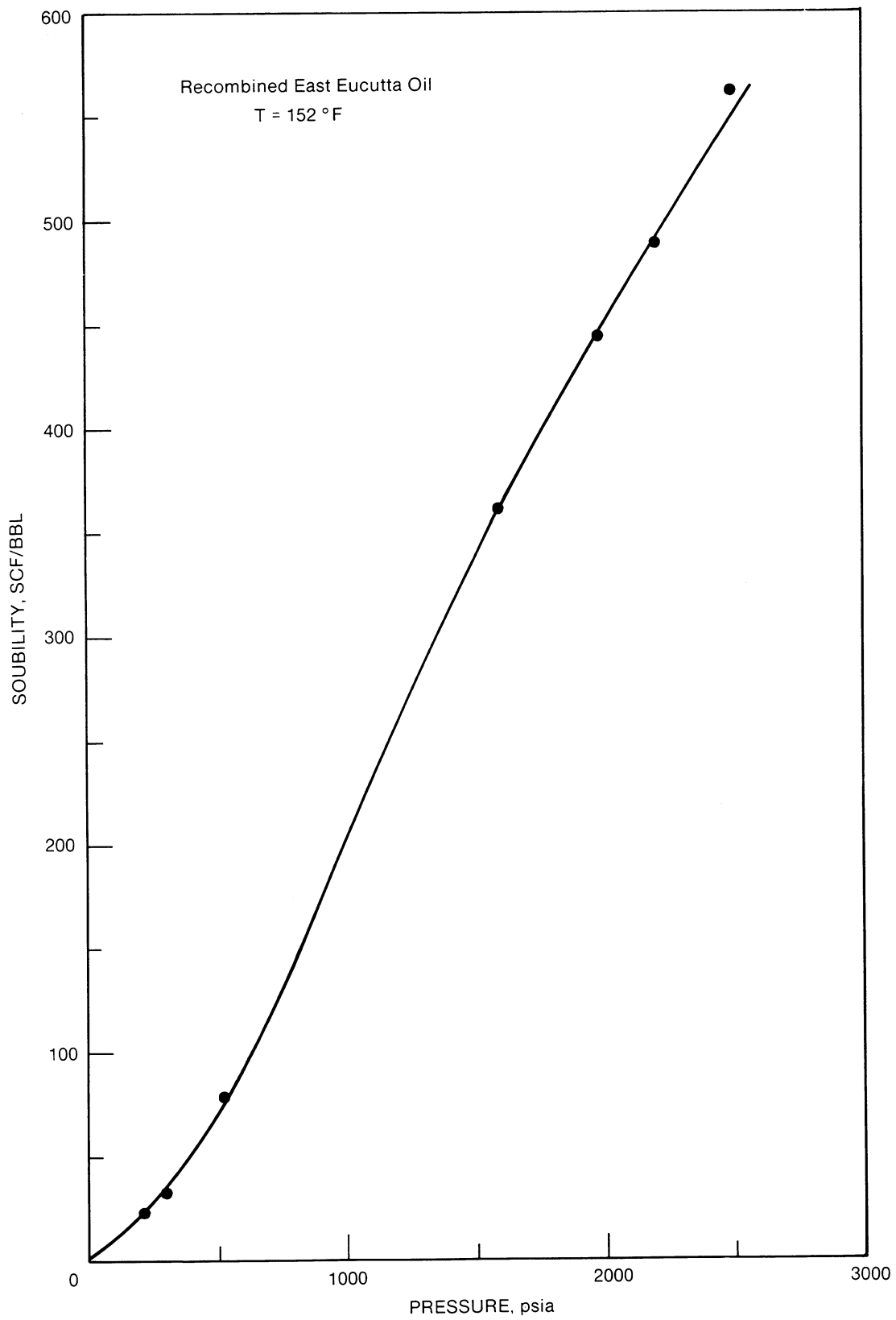


FIGURE 19. - CO₂ solubility in E. Eucutta oil.

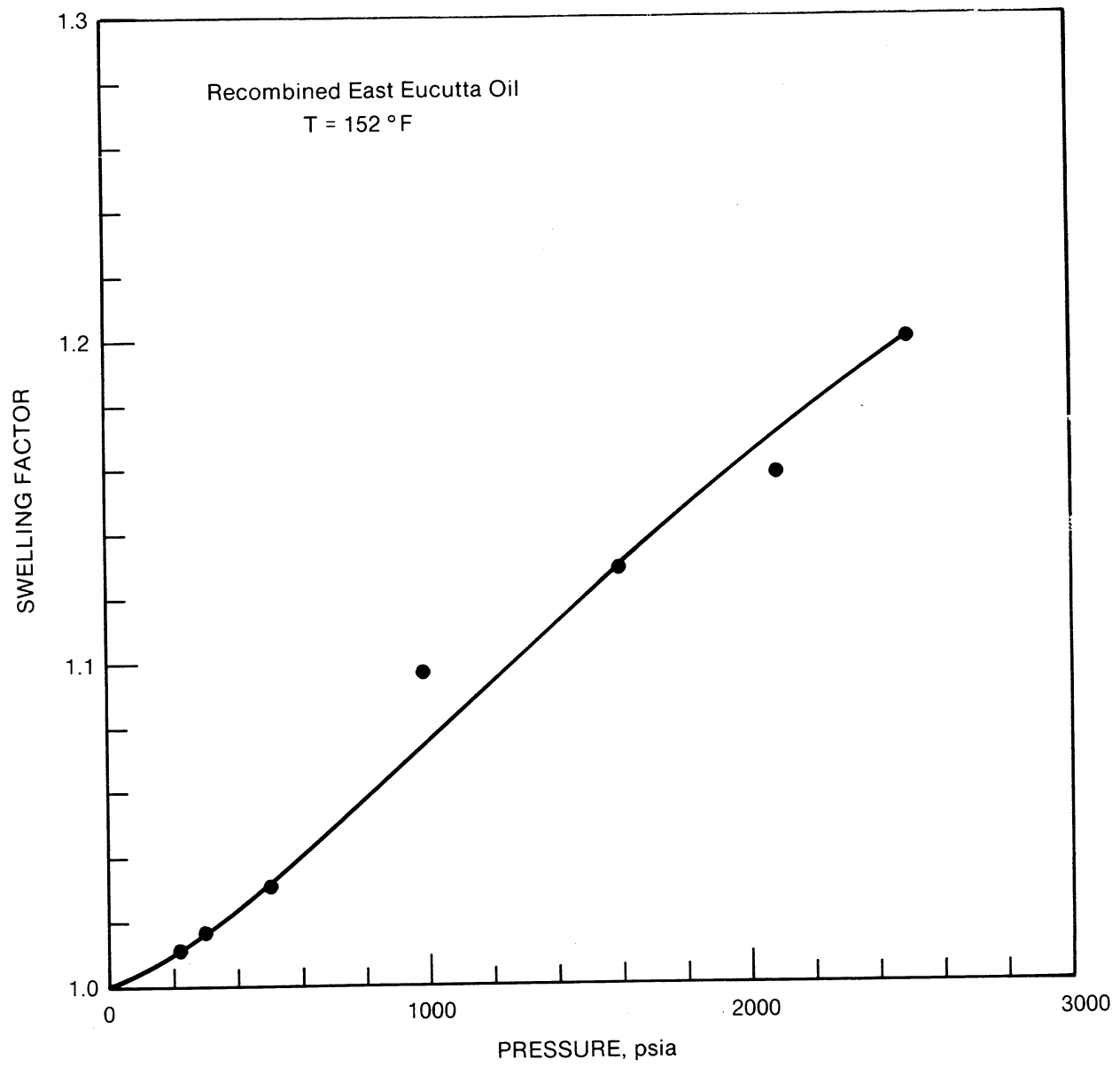


FIGURE 20. - Swelling factor for E. Eucutta oil.

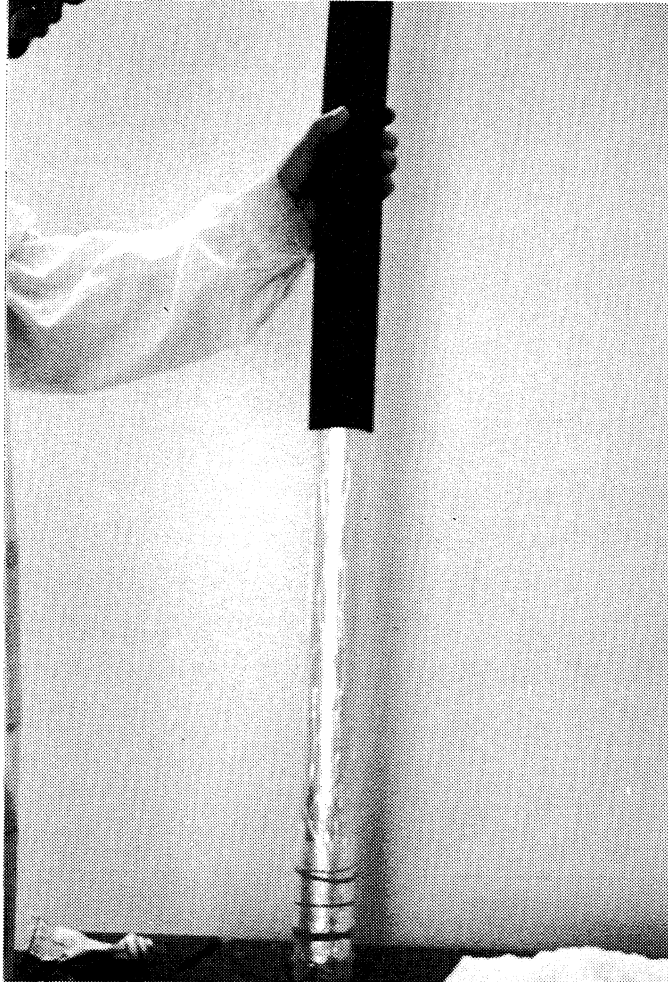


FIGURE 21. - Core wrapped with aluminum foil and rubber sleeve.

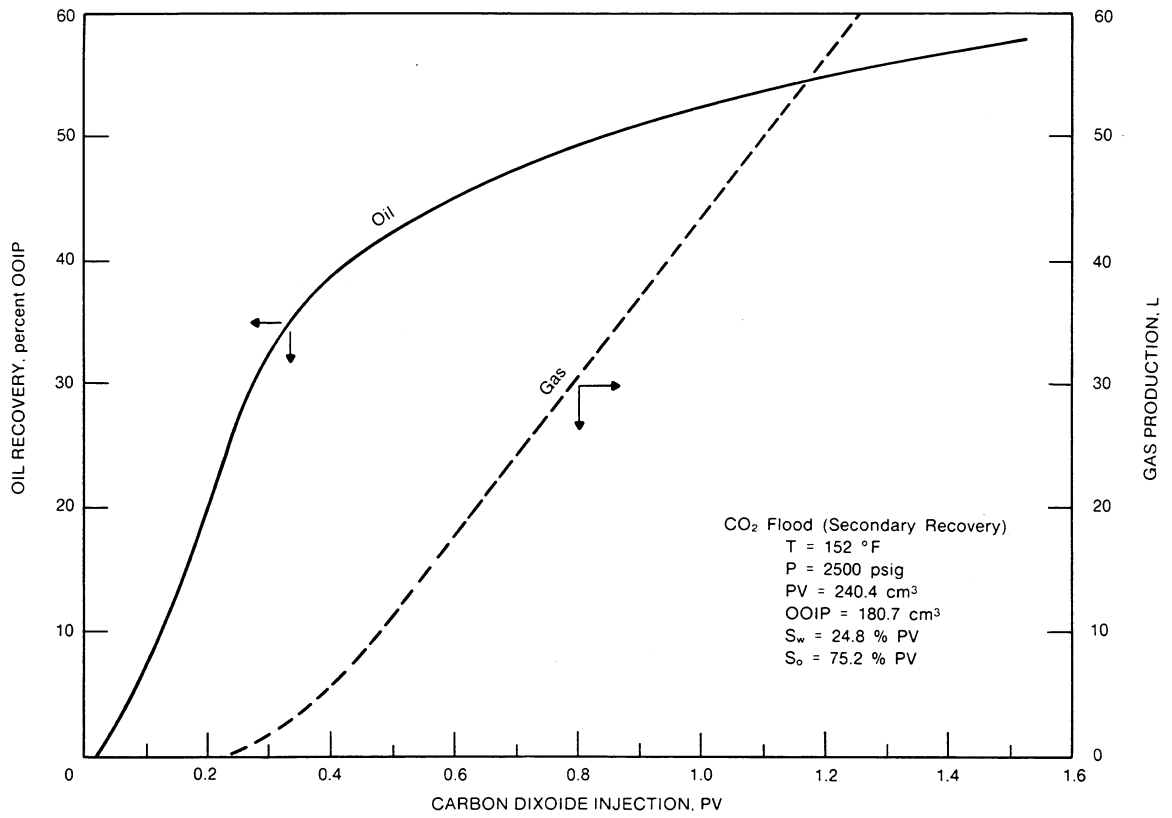


FIGURE 22. - Results from secondary CO₂ flood.

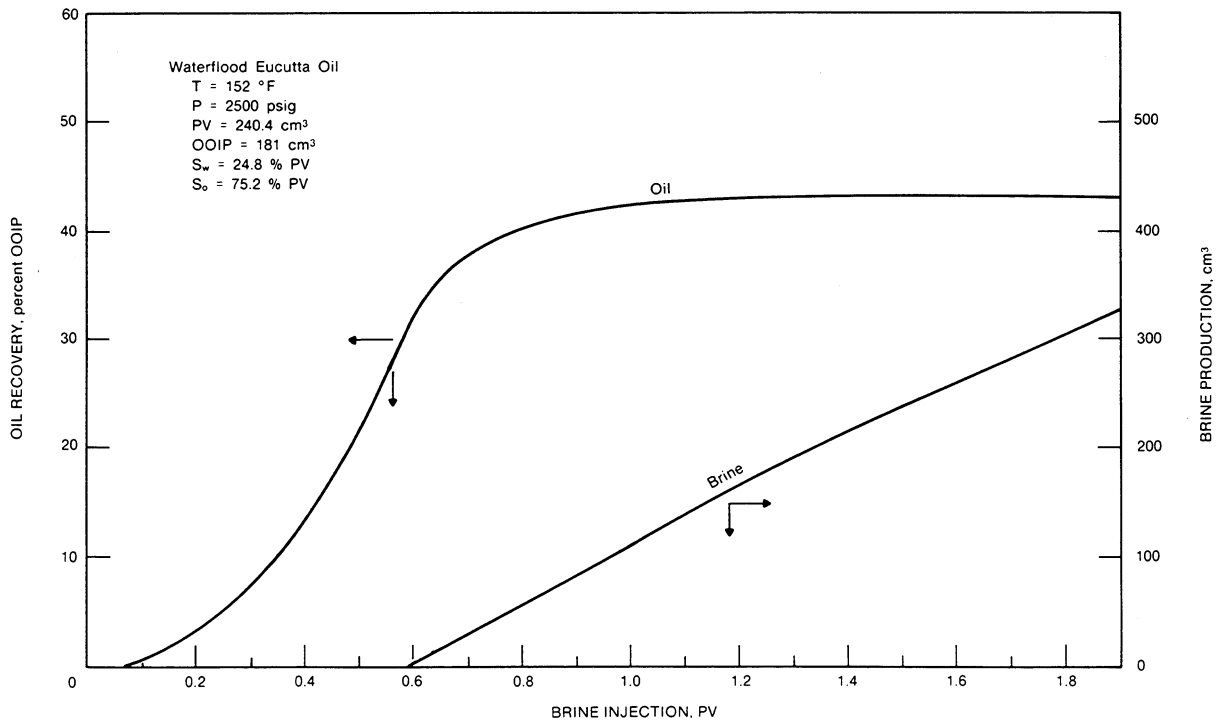


FIGURE 23. Results from waterflooding for E. Eucutta oil.

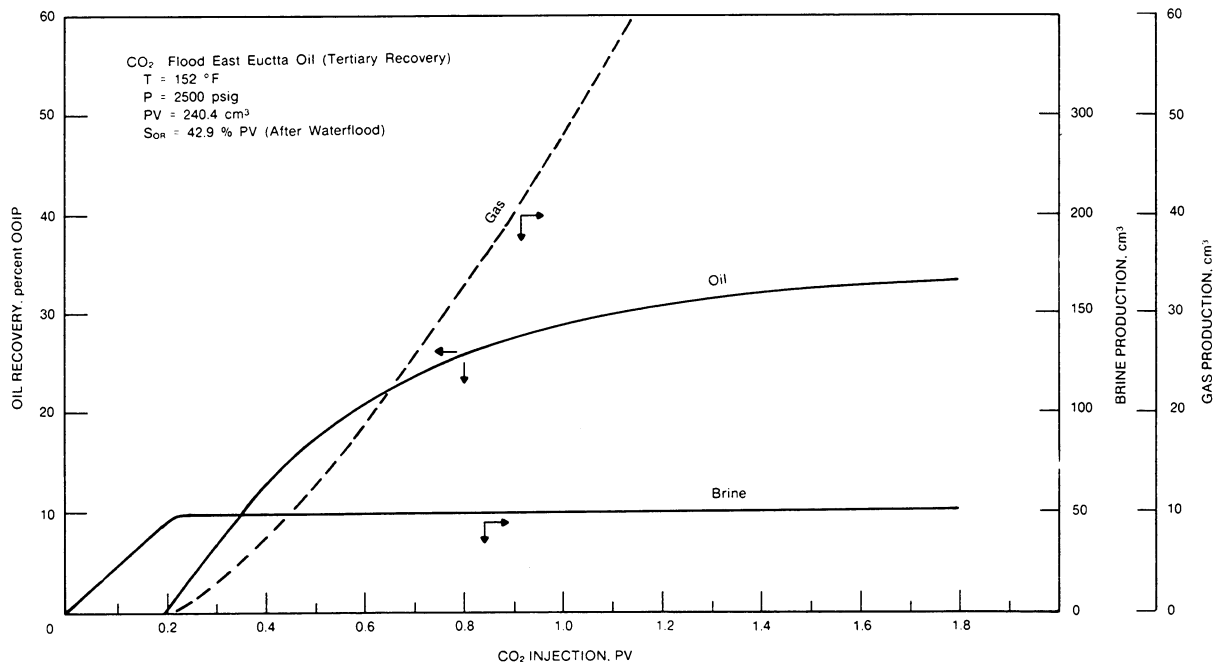


FIGURE 24. - Results from tertiary CO₂ flooding.

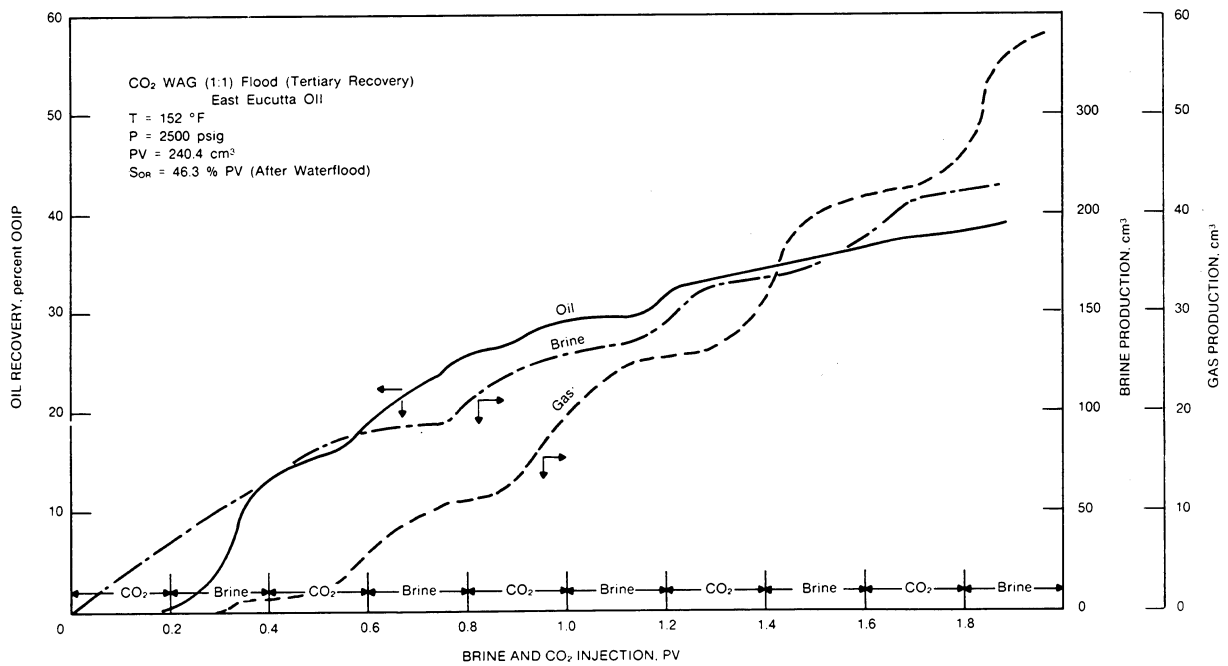


FIGURE 25. - Results from tertiary CO₂ WAG flooding.

